Mon. Not. R. Astron. Soc. **308**, 557–568 (1999)

A minor-merger model for NGC 7479

S. Laine[1]★ and C. H. Heller[2]
[1]*Department of Physical Sciences, University of Hertfordshire, College Lane, Hatfield, Herts AL10 9AB*
[2]*Universitäts Sternwarte, Geismarlandstraße 11, D-37083, Göttingen, Germany*

Accepted 1999 April 13. Received 1999 April 13; in original form 1998 October 1

ABSTRACT

The overall morphology of the barred spiral galaxy NGC 7479 is modelled in numerical simulations of a minor merger. Special attention is paid to the morphology and velocity field of the asymmetric spiral structure and the strong stellar bar. The mass of the satellite galaxy is 1/10 of the mass of the primary disc, or 1/30 of the total mass of the primary. The satellite is placed initially in a circular prograde orbit at six disc scalelengths from the centre of the primary. We follow the evolution of the merger until the secondary galaxy reaches the nuclear region of the primary. A comparison between the modelled and observed morphologies of the stellar and the ionized and neutral gas distributions and velocity fields supports the hypothesis that the transient look of NGC 7479 is a result of a minor merger. We vary several of the initial parameters of the merger and discuss their effects on the resulting morphology. The merging satellite galaxy is likely to lie within the bar of NGC 7479. We identify a possible candidate in the observational data. We discuss briefly the most probable future evolution of NGC 7479 in the light of our minor-merger simulations, and conclude that NGC 7479 is likely to evolve toward an earlier Hubble type.

Key words: galaxies: individual: NGC 7479 – galaxies: interactions – galaxies: ISM – galaxies: kinematics and dynamics – galaxies: structure.

1 INTRODUCTION

Recent observations of systems at high redshifts have produced increasing evidence that galaxy–galaxy interactions and mergers are important in shaping galaxies (e.g. Abraham et al. 1996a,b; van den Bergh et al. 1996). The Schechter (1976) luminosity function, applied to isolated spiral galaxies (Morgan, Smith & Phillipps 1998), implies an increase in galaxy number of around an order of a magnitude as the galaxy luminosity (and presumably also the mass) decreases by an order of a magnitude. Many of these lower mass galaxies are likely to be companions to more massive systems. Indeed, many companion galaxies have been detected within the gravitational influence of luminous spiral galaxies, M51 being the prime example (see also Zaritsky et al. 1993, 1997). It is plausible that close interactions, and eventually mergers, of low-mass companions (masses up to 1/10 of the primary mass) with luminous disc galaxies take place relatively frequently (see, e.g., Zaritsky & Rix 1997).

The high minor-merger rates and the important dynamical consequences of minor-mergers between luminous field spirals and their less massive companions have received more attention recently. Numerical simulations (Mihos & Hernquist 1994; Hernquist & Mihos 1995, hereafter HM95; Mihos et al. 1995; Walker, Mihos & Hernquist 1996; Thakar & Ryden 1996, 1998; Bekki 1998) have demonstrated how severely minor-mergers can affect the stellar and gas distributions, including the scaleheights and the direction of rotation. On the other hand, it has also been argued that merger events heat the discs significantly (Tóth & Ostriker 1992). In contrast, relatively little attention has been paid to the formation of tidal arms in the disc of the primary galaxy (but see Howard et al. 1993).

In this paper we emphasize the structural and dynamical consequences of a minor merger in a disc galaxy. We compare observations of the relatively nearby (32 Mpc, from the Hubble law, assuming $H_0 = 75\,\mathrm{km\,s^{-1}\,Mpc^{-1}}$ and using a recession velocity of $2371\,\mathrm{km\,s^{-1}}$; Laine & Gottesman 1998) strongly barred and asymmetric spiral galaxy NGC 7479 with numerical *N*-body models. The results from our case study help in understanding the general evolution of disc galaxies undergoing minor mergers, and should stimulate similar studies of other disc galaxies.

NGC 7479 has recently been mapped with interferometers in both its 21-cm neutral atomic hydrogen emission (Laine & Gottesman 1998) and the 2.6-mm CO emission, which traces the cold molecular gas component (Laine et al. 1999). We present images from these studies and compare them with models. NGC 7479 has strong star formation along most of its luminous western arm. In contrast, star formation on the eastern (east is to the left and west to the right in the observational images and projected

★ E-mail: seppo@star.herts.ac.uk

models) side is weak and patchy. The overall morphology is somewhat similar to NGC 2442, which has been modelled recently in an interaction scenario (Mihos & Bothun 1997). However, the arm asymmetry is even more striking in NGC 7479, and the bar much stronger and better defined.

Hα emission is relatively strong along the whole bar of NGC 7479. Vigorous star formation along the bar is observed predominantly in SBc galaxies (Martin 1995; Phillips 1996), and it may represent a relatively short-lived phase in galaxy evolution, as abundant gas along the bar is driven toward the centre (Friedli & Benz 1993, 1995; Quillen et al. 1995; Martin & Friedli 1997). NGC 7479 may be an extreme example of this galaxy type, since its strong stellar bar will drive gas inwards very quickly (Quillen et al. 1995; Laine, Shlosman & Heller 1998). The outer spiral structure is very asymmetric (Quillen et al. 1995; Laine 1996), despite the fact that the galaxy is isolated (Tully 1988). This suggests that it has gone through a very recent, and possibly still ongoing, minor-merger, as suggested by Quillen et al. This event could have triggered the asymmetric spiral arm structure, the bar formation and the gas inflow along the bar. The nucleus of NGC 7479 has been classified as a starburst based on its large and centrally concentrated 10-μm flux (Devereux 1989). However, the nuclear emission is very likely to be related to mild AGN activity rather than star formation. NGC 7479 has also been classified as a LINER (Keel 1983). General properties of NGC 7479 are listed in Table 1.

We present the numerical method employed and the initial conditions of the runs in Section 2. The comparison of the results from the minor-merger models with the observations is made in Section 3. The effects of changes in the initial conditions, evidence for a minor merger in the NGC 7479 system, the current state of the merger, and the likely future evolution are discussed in Section 4. The main results are summarized and conclusions given in Section 5.

Table 1. Some parameters of NGC 7479.

Parameter	Value
Galaxy type	SBbc(s)[a]
Environment	Isolated[b]
Right Ascension (B1950.0)	$23^{h}\ 02^{m}\ 26\overset{s}{.}36$[c]
Declination (B1950.0)	$12^{\circ}\ 03'\ 10\overset{''}{.}7$[c]
Heliocentric velocity	2371 km s^{-1}[d]
Distance	32 Mpc[e]
Linear scale	1 arcsec = 160 pc[e]
Size	4.4 arcmin × 3.4 arcmin[b]
Inclination	51°[d]
PA	22°[d]
Total *B*-band magnitude	11.60 ± .05[f]
Integrated H I flux	35.5 Jy km s^{-1}[d]
H I linewidth	345 km s^{-1}[g]
H I mass	8.6×10^{9} M$_{\odot}$[d]
^{12}CO 1–0 flux	850 ± 160 Jy km s^{-1}[h]
H_2 mass	2.5×10^{10} M$_{\odot}$[h]
IRAS 12-μm flux	1.49 Jy[h]
IRAS 25-μm flux	3.60 Jy[h]
IRAS 60-μm flux	15.1 Jy[h]
IRAS 100-μm flux	24.3 Jy[h]
L_{IR}	8.91×10^{10} L$_{\odot}$[h]
Hα flux	1.4×10^{-12} erg cm^{-2} s^{-1}[h]
Dynamical mass	2.3×10^{11} M$_{\odot}$[i]
Central activity	LINER[j]; starburst[k]
Unprojected bar length	8.6 kpc[l]
Bar axis ratio	0.41[m]

[a] Sandage & Tammann (1987). [b] Nilson (1973). [c] The radio-continuum peak (Laine 1996). [d] Laine & Gottesman (1998). [e] Assuming the Hubble law with $H_0 = 75$ km s^{-1} Mpc^{-1}. [f] de Vaucouleurs et al. (1991). [g] Huchtmeier & Richter (1989). [h] Young et al. (1989). [i] From $M = 6.77 \times 10^{4}\ R\ D\ V_{max}^{2}$ M$_{\odot}$, where R is 2.2 arcmin, D is 32 Mpc, and V_{max} is 220 km s^{-1}. [j] Keel (1983). [k] Devereux (1989). [l] Using the projected bar length of 53.5 arcsec (Blackman 1983). [m] Martin (1995).

2 METHOD AND INITIAL CONDITIONS

2.1 Numerical code

The simulations presented here were performed with a three-dimensional hybrid *N*-body/hydrodynamics code that evolves composite systems of collisionless and dissipative particles (Heller 1991; Heller & Shlosman 1994). The algorithm uses smoothed particle hydrodynamics (SPH) to model the gas dynamics. In SPH, the hydrodynamical forces are calculated as averages over local volumes defined by a smoothing length h, using a kernel interpolation. Only particles within a radius of $2h$ contribute to the sums. The smoothing length varies in space and time, and is determined by the local particle density, ensuring that the smoothed forces (pressure and viscosity) are calculated with approximately the same accuracy everywhere. The algorithm also uses a hierarchical time-stepping scheme (Whitehurst 1988). This is an important feature, since the spatial and dynamical time-scales present in the models can span many orders of magnitude. The advantages and disadvantages of SPH have been summarized by Monaghan (1992).

We assumed an isothermal state for the dissipative component with a temperature of $T = 10^{4}$ K. This results in a disc gas layer that is thinner than the stars for vertical stellar dispersions similar to the Milky Way. HM95 concluded that the gas flows in discs which are accreting small satellites are relatively insensitive to details in the equation of state if the gas can dissipate energy at the rate of a collection of colliding clouds which maintain a velocity dispersion similar to the sound speed of a 10^{4} K gas (see also Barnes & Hernquist 1996).

The total system energy (after correcting for thermal losses) and

Table 2. Initial parameters of the best model.

Parameter	Value
Number of disc star particles	80 000
Number of halo star particles	40 000
Number of satellite star particles	10 000
Number of disc gas particles	20 000
Initial distance of the satellite	6.0
Gas isothermal temperature	10 000 K
SPH viscosity coefficient α	0.5
SPH viscosity coefficient β	1.0
Initial satellite orbit	circular
Satellite orbital inclination	10°
Toomre Q-parameter	1.5
Disc star scale height	0.2
Disc gas scale height	0.057
Gas mass fraction in the disc	0.1
Gas density distribution	constant
Disc gas maximum initial radius	5.0
Disc mass	1.0
Halo mass	2.0
Halo core radius	1.0
Halo scalelength	10.0
Satellite mass	0.1
Satellite scalelength	0.15

momentum, both linear and angular, were monitored. These quantities were typically conserved to well within 1 per cent. We ran both low- and high-resolution models. For the low-N models a tree-code was used to compute the gravitational forces and SPH neighbour lists, while the high-N models were run using the special purpose GRAPE-3Af hardware (Sugimoto et al. 1990; Steinmetz 1996). The gravitational forces were softened to prevent numerical divergencies and to reduce the artificially fast two-body relaxation due to the number of particles, which is much smaller than the number of stars and gas clouds in a real galaxy. A common softening length for all dissipationless particles was used. The value of the softening length was a compromise between the values used by HM95 for the different components, i.e., disc, halo, and companion. For the dissipative particles, the softening length was set equal to the smoothing length of the hydrodynamic scheme.

2.2 Primary galaxy model

The primary galaxy model followed closely that of HM95. It employed an exponential disc of collisionless particles, with a unit scalelength. A constant surface density profile was used for the dissipative particles, which have a maximum radius of 5 scalelengths, ensuring adequate amounts of gas at the smaller radii. The z-profile followed a sech^2-law with scale heights of 0.2 and 0.057 units for stellar and gas particles, respectively. The disc is embedded in a self-consistent 'dark' halo made of collisionless particles following the density distribution given by Hernquist (1993). The halo core radius, cut-off radius and total mass are, respectively, 1.0, 10.0 and 2.0 in computational units. The Toomre Q parameter has been normalized to 1.5 at the radius of 8.5/3.5 (i.e., a Milky Way -like galaxy) and has a weak radial dependence (see fig. 1 in Hernquist 1993). In some runs we included a bulge in the primary galaxy. The spherical mass density profile of the bulge followed the one proposed by Hernquist (1990). The velocities were initialized using moments of the Vlasov equation and by approximating the velocity distributions as Gaussians. For density, velocity, epicyclic frequency and other profiles, see Hernquist (1993).

We used dimensionless units, setting the gravitational constant

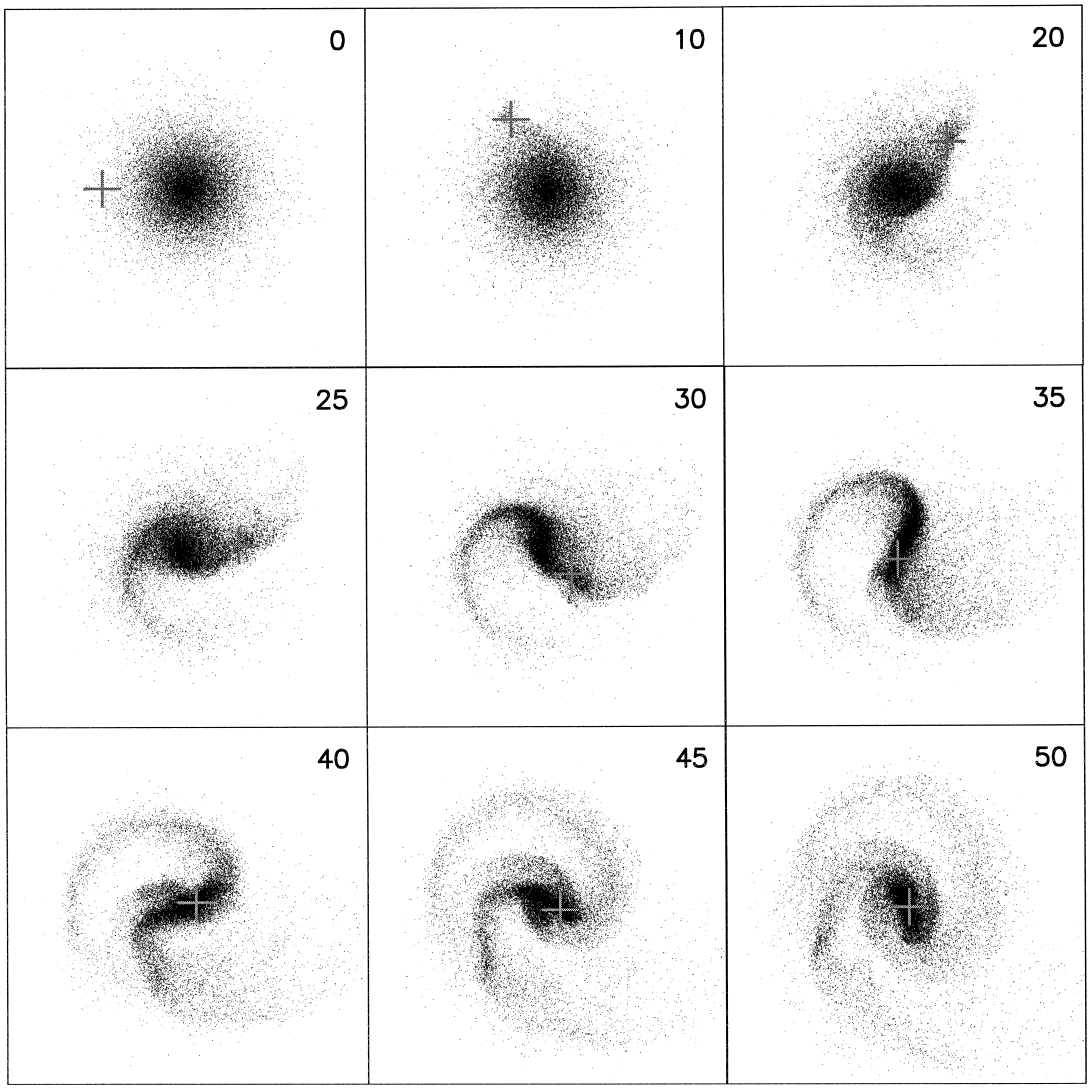

Figure 1. Evolution of the stellar distribution in the best model, seen face-on. The position of the companion is marked with a grey plus-sign. Time is marked in the upper right corner of each panel, and each panel measures 22 length units per edge. Only every third particle is plotted.

G, the disc scalelength, and the disc mass to unity. In a galaxy similar to the Milky Way, the scalelength would correspond to 3.5 kpc, the mass unit to $5.6 \times 10^{10}\,M_{\odot}$, and the time and velocity units would be 1.31×10^{7} yr and $262\,\mathrm{km\,s^{-1}}$, respectively. Our main runs were made with 80 000 collisionless disc particles, 20 000 dissipative disc particles, 40 000 halo particles and 10 000 collisionless particles for the satellite galaxy.

2.3 Satellite galaxy and encounter parameters

The satellite galaxy that we employed has a spherical bulge-like density profile (see above). The satellite scalelength was 0.15 and mass 0.1 in computational units. The mass distribution was truncated near the satellite tidal radius. We also ran models with other satellite density profiles, including a Toomre–Kuzmin disc (Kuzmin 1956; Toomre 1963; Binney & Tremaine 1987), a King density profile (King 1966; Binney & Tremaine 1987) and a $R^{1/4}$-law model (de Vaucouleurs 1948; Binney & Tremaine 1987).

Initially, the satellite galaxy was placed in a circular orbit around the primary. However, we also studied a few eccentric orbits. Results from these runs as well as the other encounter parameters are discussed in Section 3.

3 MERGER MODELS

In this section we discuss the outcome from our runs with different initial parameters. The more general aspects of physics during a minor merger have been discussed at length in HM95, and the reader is referred to that paper. Our adopted model for the primary is the same as the one used by HM95, with the exceptions of the halo mass and the gas distribution. We have reduced the halo mass by about a factor of 3 in order to allow the formation of a bar during the encounter. While the halo-to-disc mass ratio of the primary has a value of 2 globally, it is about unity within the radius of the gas disc. Test runs using the HM95 halo mass did not result in a strong bar, contrary to what is observed in NGC 7479.

We began by testing the evolution of a galaxy model in isolation. We ran a model with 150 000 particles until $t = 50$ (6.6×10^{8} yr), or for the duration of our minor-merger simulations, including gas, which comprised 1/10 of the total disc mass.

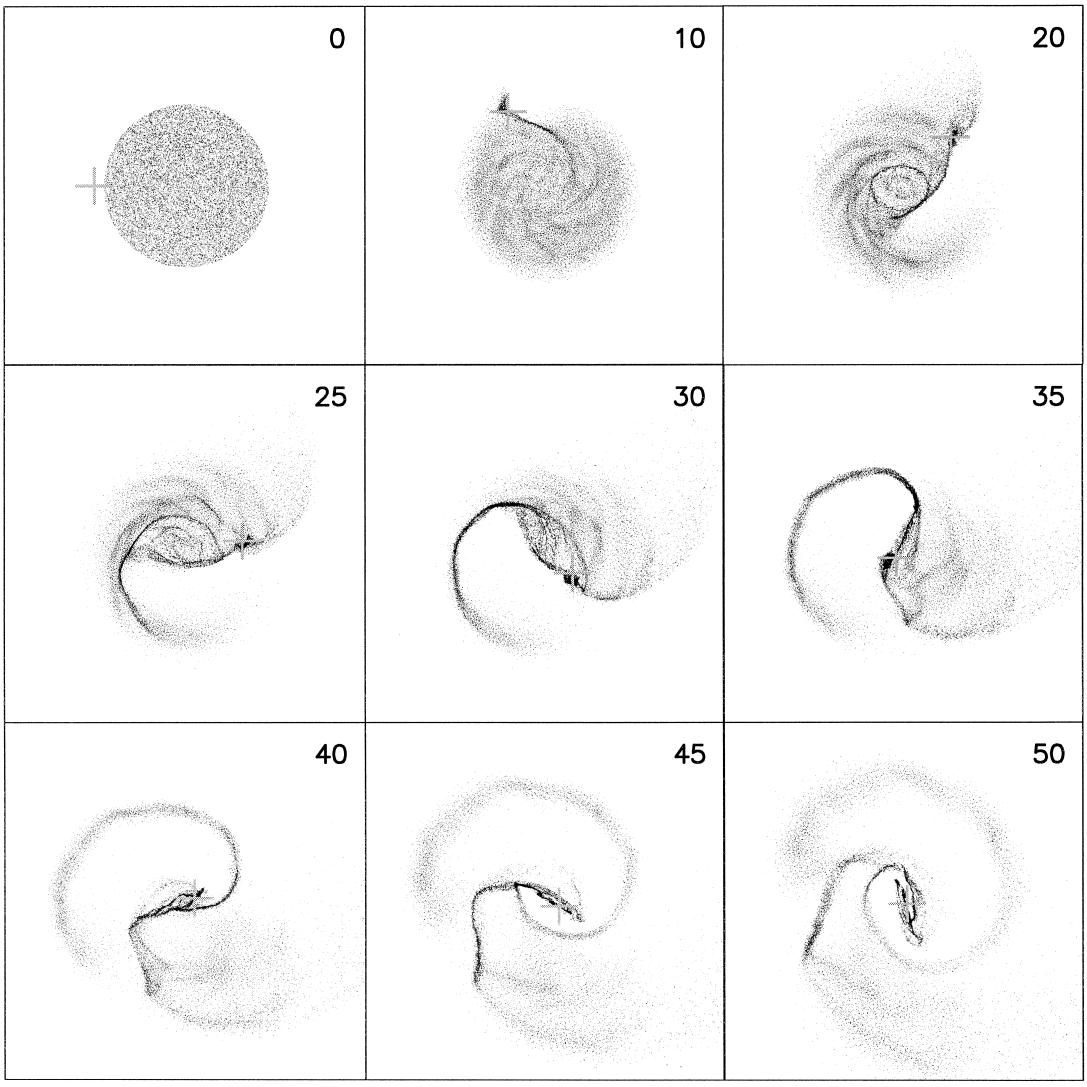

Figure 2. Evolution of the gas distribution in the best model. The position of the companion is marked with a grey plus-sign. Time is marked in the upper right corner of each panel, and each panel measures 22 length units per edge.

No bar instability, significant gas inflow or disc bending or thickening was seen, allowing us to assign any such effects to the influence of the companion in the minor-merger simulations.

From about 20 lower resolution runs, where we varied such parameters as the companion density profile, orbital inclination and eccentricity, or primary halo and bulge masses, we picked the 'best' model and ran it at a much higher resolution on the GRAPE. This model had a total number of 150 000 particles. The initial parameters are summarized in Table 2. The best model included a companion that started at a radial distance of 6 units (or 21 kpc) from the centre of the primary. Studying the merger from initial distances much larger than this using a circular initial orbit is computationally expensive. Our initial conditions are a reasonable starting point for studying the effects of an inwards spiralling satellite. Parabolic orbits and orbits with higher eccentricities will be discussed in Section 4. The satellite is initially in the plane of the disc of the primary, but its orbit is inclined to that plane by 10°. We varied the orbital inclination later to study its effect on the outcome of the merger (Section 4). A relatively small inclination is required for creation of the strong tidal features in the disc of NGC 7479.

The face-on evolution of the disc gas and stars in the best model is displayed in Figs 1 and 2. Edge-on views of the stellar disc at the start, middle and end of the simulation are shown in Fig. 3.

Figs 1 and 2 show how the companion generates a tidal arm in the main disc on the side opposite to the companion. In the time interval $t = 30$–45 the morphological appearance of the main galaxy is dominated by the tidal arm. Also, a strong bar forms in the stellar component. It is in this time interval that the structure of the simulated galaxy has many features that are seen in NGC 7479. An optical *V*-band image of NGC 7479 is shown in Fig. 4. The optical image clearly shows the luminous, long spiral arm on the western side. This arm appears to continue past the southern end of the bar and on to the eastern side. A similar morphology is seen in the simulation frames of the gas distribution after $t = 25$, as the tidal arm 'overshoots' the end of the bar and then parallels the bar until it connects to the opposite half. While the strong arm in the optical image (Fig. 4) does not appear to connect to the northern half of the bar, there is a strong dust lane about 30 arcsec north of the nucleus that connects to the bar almost at right angles, in a similar way as the gas arm in many frames of the best model. The spiral structure of NGC 7479 on the eastern side of the bar has several sections of weaker arms, similar to those seen in the model gas distribution (Fig. 2) on the side opposite to the tidal arm between $t = 25$ and 40.

The most remarkable similarity between the best model and NGC 7479 takes place at $t = 36$. To further help the comparison of the model and the observations of NGC 7479, the projected model gas particle distribution at $t = 36$ can be compared to an Hα image in Fig. 5, and the model stellar distribution with an *I*-band image in Fig. 6. The projection parameters used were (1) inclination 51°, (2) position angle of the line of nodes 22°, and (3) the angle between the bar and the line of nodes in the plane of the galaxy 25°.

Fig. 7 shows the observed line-of-sight gas velocity contours, which should be compared to Fig. 8 which shows the line-of-sight

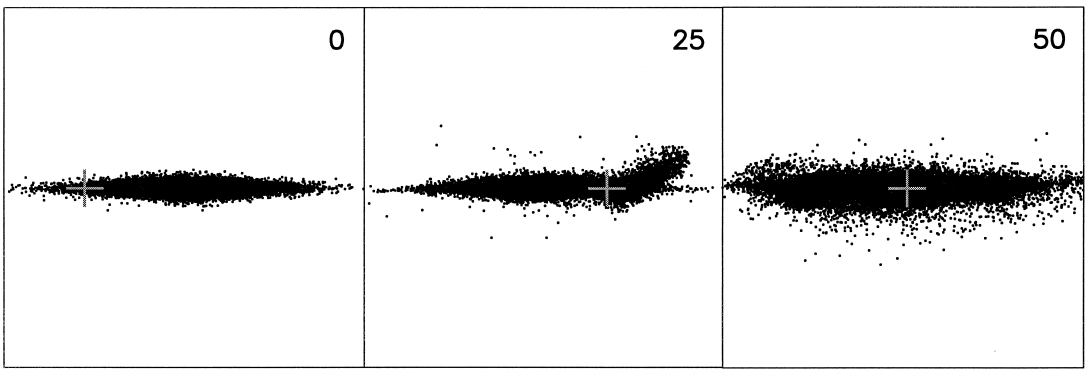

Figure 3. Edge-on view of the evolution of the stellar distribution in the best model. The position of the companion is marked with a grey plus-sign. Time is marked in the upper right corner of each panel, and each panel measures 20 length units per edge. Only every third particle is plotted.

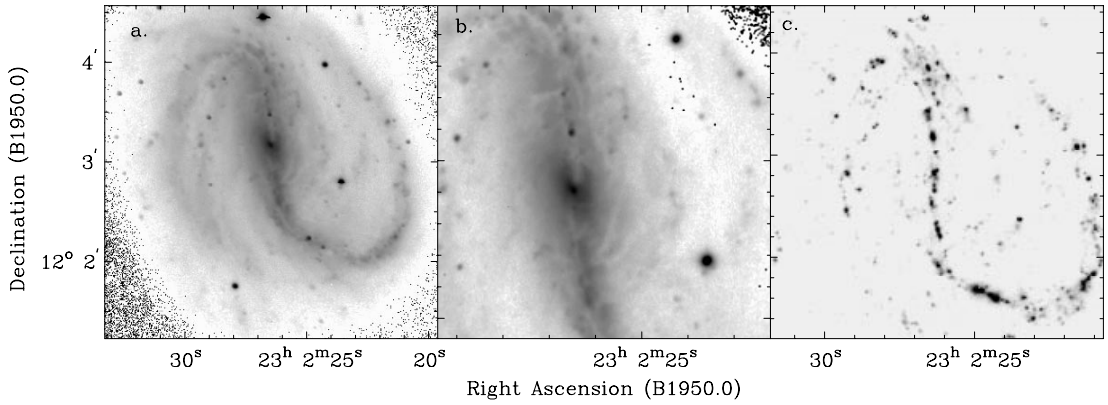

Figure 4. (a) Optical *V*-band image of NGC 7479, showing the star-forming and dust spirals. (b) Optical *V*-band image of the central bar region of NGC 7479. The dust lanes are easily seen in this image. (c) A high-resolution (0.8 arcsec) Hα image of NGC 7479.

velocity field of the projected model frame at $t = 36$. Even with 20 000 gas particles, the simulation suffers from a lack of particles in the area between the tidal arms. Because of this, only a few line-of-sight velocity contours are drawn in Fig. 8.

An additional interesting feature can be seen in the projected gas density (Fig. 5). A relatively sharp turn occurs in the strong spiral arm towards the lower right of the galaxy centre. A similar sharp bend is visible in the observations, although it takes place a little further south. It is most easily seen in the H I distribution (Fig. 7). It is also striking that the simulation frames reveal a thicker, 'lens-like' feature around the bar in the stellar distribution, bracketed by the curved extensions of the gaseous spiral arms outside the bar. A similar feature was seen in the colour index images of NGC 7479 (Quillen et al. 1995; Laine 1996), reproduced here in Fig. 9.

The companion in our runs was not disrupted during its spiralling descent into the nucleus of the main galaxy. As an example of the appearance of the companion, we show the companion particles plotted with a light grey colour on top of the stellar particles at $t = 36$ in Fig. 10. It is also obvious from this figure that the stellar surface density at a given radius in the bar is higher on the side opposite to the companion than on the side close to the companion. A similar asymmetry can be seen in *K*-band images of the bar, which show the southern bar to be systematically brighter by about 0.2–0.3 mag. In addition, there is a knot in the bar in the *K*-band image at about 17 arcsec north of the nucleus, as can be seen in Fig. 11. The relevance of this knot to the remains of the merged galaxy is discussed in Section 4.

The model velocity field shown in Fig. 8 reveals the 'tongues' of velocity contours on both sides of the bar, one reaching from the bottom upwards on the right side of the bar, and the other reaching from top downwards on the left side of the bar. Similar 'tongues' occur in the Hα velocity field shown in Fig. 7. Such 'tongues' form when there is a strong radial component in the gas flow as in the case of gas orbits elongated along a strong bar. Another striking similarity is seen in the northern arm section, where the velocity contours in both the observations (H I) and models have abrupt bends toward lower and higher velocities,

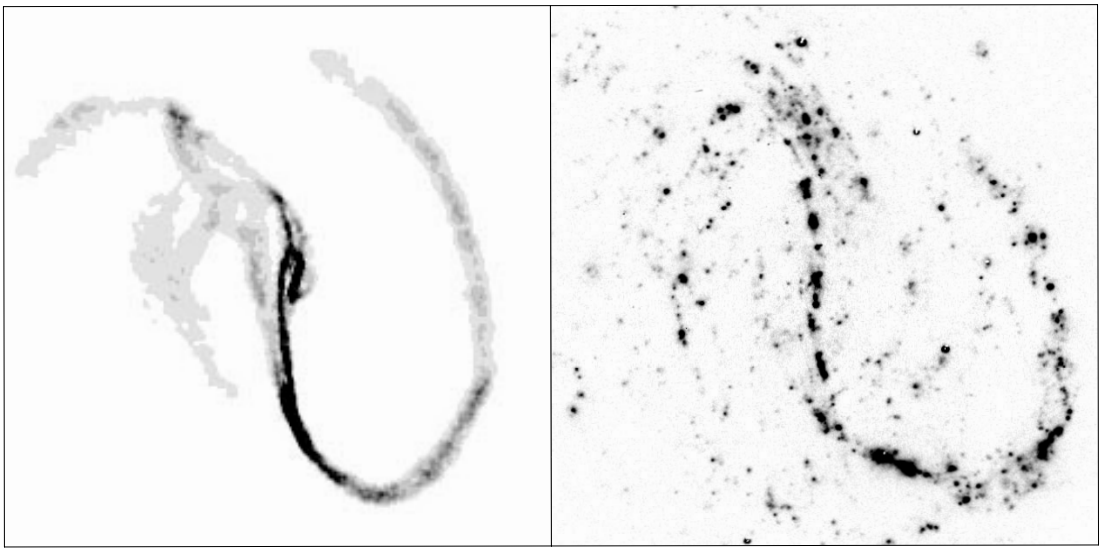

Figure 5. The model gas distribution at the best matching time, $t = 36$ (on the left), compared to the observed Hα image of NGC 7479 (on the right).

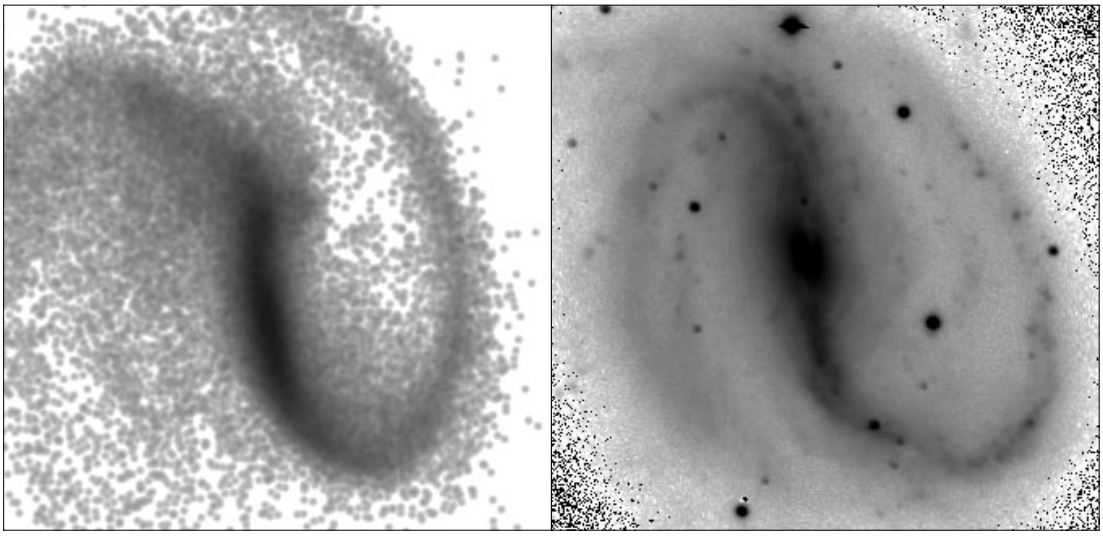

Figure 6. The model star distribution at the best matching time, $t = 36$ (on the left), compared to the observed *I*-band image of NGC 7479 (on the right).

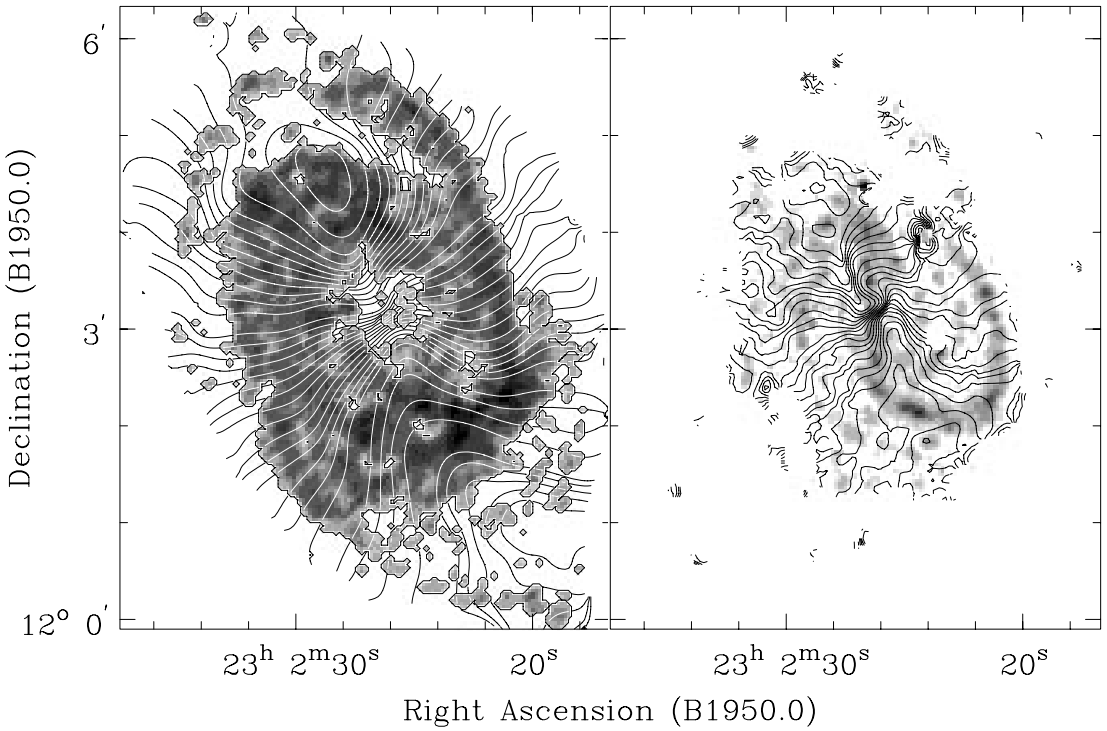

Figure 7. (a) NGC 7479 21-cm H I integrated intensity at 8.5-arcsec resolution (grey-scale) with 30-arcsec resolution line-of-sight velocity contours drawn on top at 10 km s^{-1} intervals. (b) Hα emission grey-scale image of NGC 7479 at 3.5-arcsec resolution with 12-arcsec resolution line-of-sight velocity contours drawn on top at 12 km s^{-1} intervals (the unpublished Hα data were kindly given to us by S. Vogel and M. Regan).

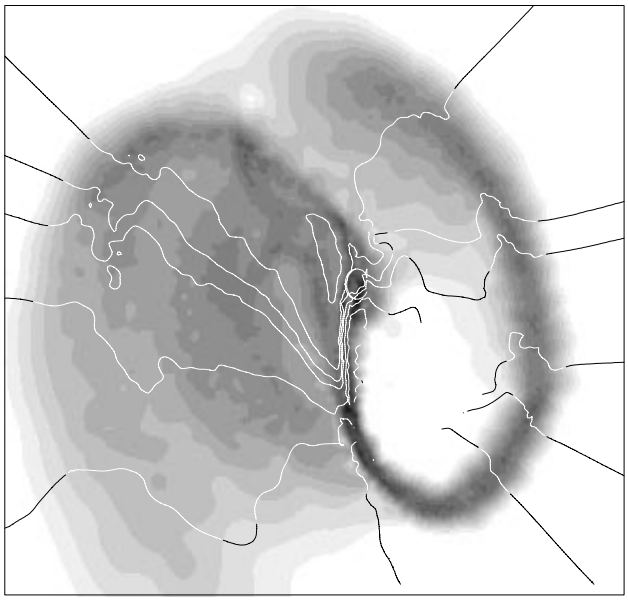

Figure 8. Grey-scale image of the projected model gas distribution at $t = 36$ in the best model, with some projected line-of-sight velocity contours overlaid.

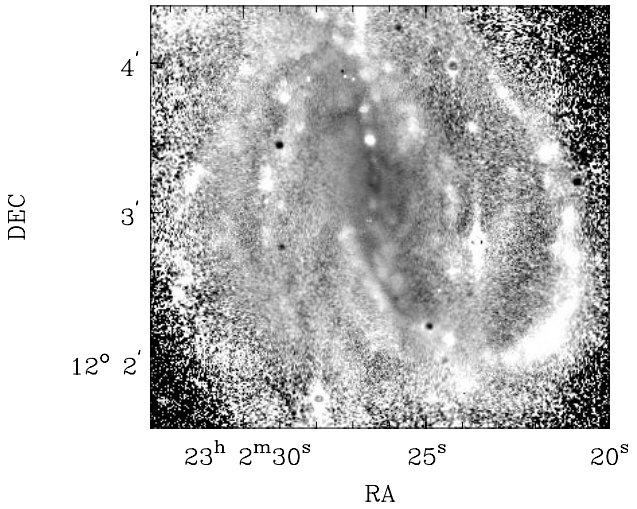

Figure 9. $B - V$ image of NGC 7479, showing the redder (darker shades) region around the bar, bounded by bluer colours (lighter shades).

depending on which side of the kinematical major axis they lie. The model velocity plot shows that the particles which form the arm have a substantial non-circular velocity component; the strong arm is a material arm responding to the tidal perturbation and 'sweeping' outwards (Fig. 12). When comparing the velocity figures it should be kept in mind that the projected velocities were evaluated using the SPH formalization, which involves a two-dimensional kernel and a smoothing length which defines the effective spatial resolution and is dependent on the particle density. Therefore the spatial resolution in the velocity image is higher in regions which are densely populated with gas particles (which in this case also means higher gas surface density). In this way the evaluations are consistent with the hydrodynamic approach and also result in similar accuracies everywhere.

The edge-on views of the disc presented in Fig. 3 demonstrate that the minor-merger has not caused thickening of the disc by more than a factor of 2, consistent with the results of Quinn, Hernquist & Fullagar (1993) and Walker et al. (1996). The

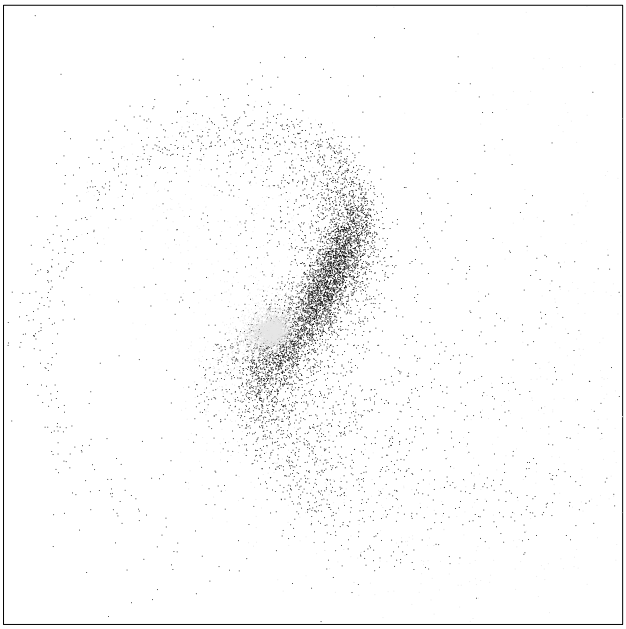

Figure 10. Particle plot showing the stars in the primary galaxy and the companion. Every 6th particle of the primary stars is plotted. The companion is shown in light grey colour.

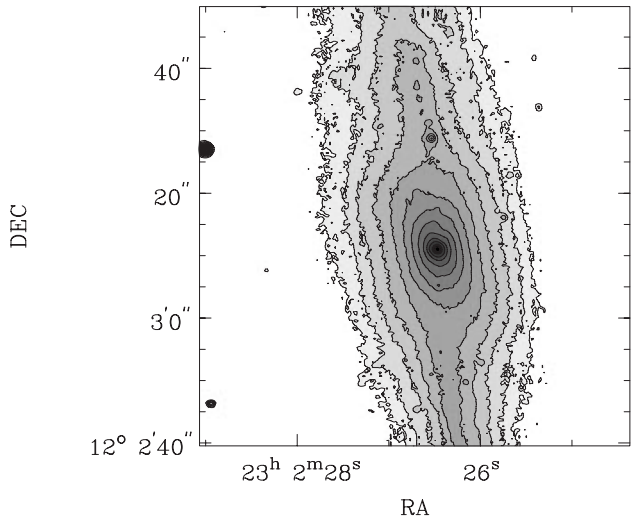

Figure 11. *K*-band image of the bar in NGC 7479, showing the knot in the bar 17 arcsec north of the nucleus.

thickening of the disc (and the concomitant increase in stellar velocity dispersions) has evolved the model towards the characteristics of an earlier Hubble-type galaxy.

4 DISCUSSION

As discussed below, there are no interaction candidates around NGC 7479. However, the results presented in Section 3 are consistent with the merger hypothesis. The main features present in our model include a strong one-armed structure, and the long bar near the centre of the disc. Features in the model velocity field are also consistent with the minor-merger hypothesis. The big challenge of the merger hypothesis is to explain what has happened to the perturber of the NGC 7479 system.

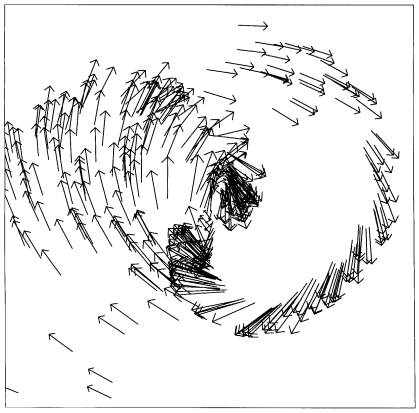

Figure 12. Face-on-plot of unprojected velocity vectors of the best model at $t = 36$. The bar is oriented vertically, and the dominating tidal arm is on the right. The lengths of the velocity vectors are proportional to the particle speeds.

4.1 Evidence for a minor-merger in the NGC 7479 system

4.1.1 Introduction and related earlier work

What has caused the remarkable asymmetry in the spiral arm structure of NGC 7479? In principle, this could be a result of the intrinsic evolution of the disc in isolation. Earn (1993) has studied the maintenance of one-armed patterns in spiral galaxies. He concluded that the rotation curves need to have the correct form to support one-armed patterns. Specifically, if $\Omega(r) - \kappa(r)$ is constant over a large range of radii, a one-armed spiral can be maintained. Here $\Omega(r)$ is the angular velocity corresponding to the galaxy rotation curve, and $\kappa(r)$ is the epicyclic frequency, both being functions of radius. We have applied this test to the H I rotation curve (Laine & Gottesman 1998) of NGC 7479. It turns out that this quantity is not constant anywhere in the disc where the rotation curve can be determined, but rather varies proportionally to the radius. Even if the disc rotation curve was capable of maintaining an $m = 1$ perturbation, the question of the origin of the asymmetry remains. Probably interactions are responsible for exciting many if not all the strong $m = 1$ asymmetries observed, as in the Magellanic-type galaxies (Odewahn 1994, 1996). A recent interaction or merger is the most likely explanation for many of the prominent features seen in NGC 7479.

A relatively recent study of one-armed spiral galaxies was made by Phookun (1993). He studied a sample of five one-armed spiral galaxies, NGC 3162, NGC 4027 (Phookun et al. 1992), NGC 4254 (Phookun, Vogel & Mundy 1993), NGC 4654 (Phookun & Mundy 1995) and NGC 5713. It turned out that every one of these galaxies is interacting with the environment, usually with a companion galaxy or a large H I cloud. There is no evidence for a lack of a massive halo in any of these galaxies. In the absence of a massive halo, the $m = 1$ perturbations are favoured in the scenario of swing amplification (Toomre 1981; Carlberg & Freeman 1985).

4.1.2 Observational evidence for a recent merger in NGC 7479

Some evidence for a recent interaction or merger in the NGC 7479 system comes from the high-resolution H I observations. They show a long gaseous arm (Fig. 7) that seems to have kinematics different from those of the main gas disc. An intrinsic H I warp can

in principle produce the observed peculiar kinematics, but there is no integral sign -like form, or any other symmetry in the kinematical warp, contrary to what is usually observed in warped galaxy discs. The kinematics of the gas arm are, however, consistent with radially expanding motion in response to a tidal perturbation.

The optical images of NGC 7479 show a strong one-armed spiral pattern on the western side, with irregular short armlets on the opposing side. These observations are most naturally explained by a minor merger. The simulations presented in this paper suggest that the merger is relatively recent or ongoing, and its effects should be still easily visible, due to the large dynamical time-scale for mixing in the outer disc, where most of the arm structure lies. The optical image (Fig. 4) also shows an anomalous pattern of dust lanes perpendicular to the bar and the south-west spiral arm, often connecting to Hα emission in the bar or the spiral arm. In the minor-merger scenario, the dust trails may be associated with stripped clouds from the merging companion, as the dust lanes in the nuclear region of M31 (Sofue 1994).

Besides the strong concentration of molecular gas in the nucleus, molecular gas is also found along the bar (Laine et al. 1999). This suggests that something has recently triggered a still ongoing gas flow into the nuclear region. The gravitational perturbations generated by a satellite galaxy, including a recently created bar, can explain the transient look of the CO emission in NGC 7479. The lack of strong star formation in the centre also suggests that the nuclear pile-up of gas has been relatively recent, and therefore the bar is relatively young. Finally, P. Martin (private communication) has made optical spectral measurements of several H II regions in NGC 7479, and his preliminary results indicate that the [O III]/Hβ ratio is considerably higher in the western arm than on the eastern side of the galaxy. This ratio reflects both the excitation conditions ([O III] is a high-excitation line) and the element abundance ratios, and thus metallicities. While there may be several possible explanations for the difference in this ratio along the arms of NGC 7479, the ratio is consistent with the existence of strong shocks along the western arm produced by recent tidal effects and shocks that form when a tidal arm sweeps the gas in a disc (cf. NGC 2442; Mihos & Bothun 1997).

4.2 Current state of the merger

The observations and their comparison to the simulation frames suggest that the merger is not complete, but the remains of the satellite galaxy are likely to lie at some distance outside the nuclear 1–2 kpc region. No interacting companion galaxies within 12 arcmin or $\pm 440\,\mathrm{km\,s^{-1}}$ of the centre of NGC 7479 have been found in deep H I or optical observations (Laine & Gottesman 1998; G. F. Benedict, private communication). Palomar Sky Survey prints show that the nearest recognizable galaxy lies almost 1°, or about 500 kpc, away from NGC 7479. Therefore any companion of NGC 7479 is likely to lie within the disc of NGC 7479.

It is important to note that under reasonable initial conditions the companion in our simulations is never completely disrupted. A careful inspection of the disc of NGC 7479 reveals evidence for the still-intact remains of a companion. At $t = 36$ in the best model, the companion is on the leading edge of the bar, about a half bar radius from the nucleus (Fig. 11). Images of NGC 7479 in fact reveal a point-like object near this location, about 17 arcsec north of the nucleus, seen in the optical (including Hα; Figs 4, 5 and 7), near-infrared (Fig. 11) and CO images (Laine et al. 1999). The radio-continuum image presented by Laine & Gottesman (1998) has a peak near this location as well, but displaced to the west. The point 17 arcsec north of the nucleus is associated with a relatively strong perturbation of the Hα velocity field (Fig. 7). The constant-velocity contours in Fig. 7 bend into the bar from the western side at this location. A similar morphology does not exist at the corresponding location on the southern section of the bar. The gas in this location is likely to have a large radial infall velocity (Laine et al. 1999).

The strong Hα emission in the western arm and the abundant star formation and molecular gas along the bar are consistent with the idea that a minor-merger is still progressing. The gas is compressed in the tidal arm and becomes susceptible to star formation. The tidal arm in our simulations becomes weaker once the companion falls deep into the bar region, implying that the strong starburst in the western arm of NGC 7479 may become considerably weaker within the next 10^8 yr.

4.3 Future evolution of NGC 7479

The bar in our simulations forms rapidly, during about 10 time units, which corresponds to less than 1.5×10^8 yr if we use the physical units of HM95. After another 1.5×10^8 yr the bar is destroyed as the companion spirals into the nucleus. In NGC 7479, the bar destruction is likely to take place relatively soon, within a few 10^8 yr, since the companion appears to be in the bar relatively close to the nucleus at the current time, as argued above. The massive concentration of molecular gas in the nucleus of NGC 7479 is likely to increase and trigger a nuclear starburst, possibly creating a more massive stellar bulge and, eventually, also weakening the bar. The tidal arm becomes weaker in time, and star formation is likely to decrease in the tidal arm once the companion has reached the nuclear 1–2 kpc region. Thus it is likely that NGC 7479 is evolving towards an earlier Hubble-type galaxy, in accordance with the theory of secular dynamical evolution (e.g. Martinet 1995).

Some uncertainty into our modelling and predictions for the future dynamical evolution of NGC 7479 is brought about by the unknown effects of star formation. These issues will have to be dealt with in future studies if further progress is to be made.

4.4 Effects of changes in the initial conditions

So far we have addressed only a very specific set of initial conditions. In the following we will discuss how various changes in the initial conditions affect the structural and kinematical evolution of a minor-merger.

The various parameters whose influence we investigated are given in Table 3. These test simulations were made with only about 12 000 total particles to save computational time, allowing a greater range of parameters to be explored. Even with the reduced number of particles, the overall structures can be studied relatively reliably.

As noted by HM95, a considerable fraction of the satellite is likely to survive a merger if its average mass density is higher than that of the disc and halo. We have run several cases of differing average mass densities for the satellite, varying its mass from 0.05 to 0.1 and the scalelength from 0.1 to 0.9. The bulk of the companion is not disrupted, except in the extreme cases when

Table 3. Various parameter values whose influence on the merger morphology was studied.

Parameter	Value
Companion density profile	King profile
Companion density profile	Toomre–Kuzmin disc
Companion density profile	de Vaucouleurs $R^{1/4}$ law
Initial distance of companion	8.0
Companion orbit	eccentric ($e = 0.2$, 0.3, 0.5, parabolic)
Companion orbital inclination	0°, 30°
Gas mass fraction in the disc	0.2
Gas density distribution	exponential
Halo mass	5.8
Satellite mass	0.05–0.1
Satellite scalelength	0.1–0.9
Primary galaxy structure	inclusion of a bulge

unrealistically large scalelengths (0.9) were used. In every realistic case, most of the companion survives the plunge into the nucleus of the primary. Even companions with mass ~ 0.05 are able to produce many of the observed features of NGC 7479. We also used other density profiles for the companion, including the Toomre–Kuzmin model (Kuzmin 1956; Toomre 1963; Binney & Tremaine 1987), the King density profile (King 1966; Binney & Tremaine 1987) and a $R^{1/4}$-law model (de Vaucouleurs 1948; Binney & Tremaine 1987). Using a realistic scalelength or size for the companion, in combination with these other mass density profiles, did not change the outcome significantly. We conclude that if NGC 7479 has experienced a minor-merger with a satellite galaxy which has 5–10 per cent of the primary disc mass, the companion has probably not been fully disrupted.

While we do see some features possibly related to the remains of a companion in the disc of NGC 7479, they are not striking in optical and H I images. If part of the companion mass consists of gas particles, it helps a little in making it more susceptible for disruption, but even with a gas mass fraction of 50 per cent, the bulk of the companion is not disrupted (Laine 1996). It is possible that the majority of the mass of the companion is dark matter, as some studies (see Ashman 1992, and references therein) have shown that the fraction of 'dark matter' increases with decreasing galaxy mass, and the dark mass can be up to dozens of times the visible mass in dwarf galaxies. It is conceivable that dark matter dominates the mass of the companion. Therefore one would not necessarily expect to see a luminous blotch at the current location of the companion.

Changing the halo mass fraction to a larger value, 5.8 times the disc mass (as used by HM95), resulted in a merger where the formation of the bar was suppressed. This is the well-known result of massive haloes suppressing the formation of a bar (see, e.g., Ostriker & Peebles 1973). The remarkable thing is that even forcing by a relatively massive merging companion is incapable of inducing a well-formed bar when the halo mass is high.

A similar result was obtained when we employed a moderately massive spherical bulge component with one-third of the disc mass. Again, the bar did not form. The bulge can destroy the orbital support for a bar and cause chaos in the inner radii (Hasan & Norman 1990; Friedli & Benz 1993; Norman, Sellwood & Hasan 1996).

Reducing the encounter inclination to 0° gave essentially the same results as the 10° inclination. With an elevated inclination of 30°, the companion was first dragged into a low-inclination orbit at a large radius, in accordance to the results of Walker et al. (1996). The subsequent evolution followed that seen in our standard models, although a better match with the observed morphology was obtained with the lower inclinations. Thus our results are not very sensitive to the initial orbital inclination of the satellite galaxy, as long as it is not too large. However, the 30° inclination encounter did produce a significantly larger perturbation of the outer disc in the z-direction. It is difficult to estimate whether the disc of NGC 7479 currently has a large z-thickness.

Using a primary gas distribution which is initially exponential instead of flat resulted in more gas in the bar. The outer arm regions were less populated and thus less well-defined. However, the overall morphological evolution was very similar to that of a constant density gas disc. Increasing the gas mass fraction of the primary disc from 0.1 to 0.2 caused the gaseous disc to produce stronger arms at early times, and a relatively strong two-armed structure appeared, which is inconsistent with the observations of NGC 7479. We conclude that the primary disc gas mass fraction is not likely to be as high as 0.2.

We also made some runs with the companion starting at an initial distance of 8 units. In this case the generation of the bar and the asymmetric spiral structure were delayed, as expected, but once the companion fell to a radial distance of 2–3 from the primary centre, the bar and the tidal arm formed in much the same way as in our best model. In addition, the structure on the side opposite to the main tidal arm was very similar.

Effects of the initial orbital eccentricity were studied by giving the companion initial velocities that corresponded to orbital eccentricities of 0.2–0.5. We also studied parabolic orbits where the companion started at a distance of 12 units from the centre of the primary. Various impact parameters were also tried, varying from twice the disc scalelength out to perigalacticon distances beyond the gas disc radius.

In cases where the companion starts on a parabolic orbit, it passes through the disc without merging during its first plunge. When the perigalacticon was very close to the centre of the primary (two disc scalelengths), the companion comes back after a relatively short time and then merges rapidly. At no point during this simulation did the observed stellar or gas distribution assume a morphology similar to the observations. The first pass of the companion through the disc causes only patchy structures, and the subsequent merging during the second plunge takes place so rapidly that the companion does not have time to drive bar and tidal arm formation. The simulations with the companion passing at larger distances through the disc in a parabolic orbit did not result in a significant slowing down of the companion, and we did not continue the simulations to follow the second plunge.

We also ran simulations where the companion started at a distance of 12 units and had eccentricities of 0.3 and 0.5. The more eccentric case produced a rapid merger, and again the companion did not have time to drive the formation of a bar or a strong tidal arm. Therefore such a high eccentricity is likely to be inconsistent with the observed morphology of the NGC 7479 system. The more moderate eccentricity of 0.3 produced a merger at a lower pace, and the companion had enough time to drive the formation of a stellar bar and a moderately strong tidal arm. However, the bar was shorter than in cases where the merger took place from a circular initial orbit, and the match of the overall structure, including the tidal arm, to the morphology of NGC 7479 was not as good as for our best model (with a circular initial orbit).

Therefore, although a comprehensive study of the parameter space of initial conditions is left for a future paper, we conclude that mergers from moderately eccentric orbits of a companion ($e < 0.5$) are consistent with the observed morphology of NGC 7479. Such interactions are possibly seen elsewhere in the nearby Universe. The prime example is M51 and its companion NGC 5195, which may be in a bound orbit, destined to merge relatively soon (Howard & Byrd 1990; see also Salo & Byrd 1994). In the future, we plan to make a more comprehensive study of minor-mergers by sampling the parameter space of initial conditions more densely. Also, the NGC 7479 system represents a good case for the use of a genetic algorithm to extract and refine the initial conditions that lead to the observed morphology of the system (Theis 1998).

5 CONCLUSIONS

We have performed simulations of minor-mergers between satellite galaxies with masses 5–10 per cent of the disc mass of the primary galaxy and primaries which have a halo mass twice their disc mass. We compared the results from these simulations to the various observations of NGC 7479, testing the hypothesis that NGC 7479 has undergone a recent minor merger which may not be complete. The results suggest that companions of moderate mass, merging from orbits with eccentricities < 0.5, can reproduce most of the salient observational features of NGC 7479, including (1) a strong stellar bar; (2) a strongly asymmetric spiral arm structure in the gaseous and stellar distribution of the primary, specifically a strong tidally induced arm; (3) many features of the line-of-sight velocity field; (4) the concentration of molecular gas into the nuclear zone and along the bar, and (5) the various anomalous dust lanes that cross the disc and the bar.

The simulations also suggest that the companion has not been completely disrupted. The best candidate for the current position of the remains of the companion is the feature about 17 arcsec north of the nucleus. This feature can be seen in the optical and near-infrared broad-band images, CO emission, Hα images, and as a perturbation in the CO and Hα images of the line-of-sight velocity fields.

The future evolution in the NGC 7479 system is likely to lead to an increasingly large central concentration of molecular gas, and the resulting nuclear starburst could create a more massive bulge. Together with the addition of the remains of the satellite galaxy, the increased central mass concentration is likely to eventually destroy the stellar bar, and the overall appearance may then resemble an earlier Hubble-type galaxy.

ACKNOWLEDGMENTS

SL thanks the help and advice of Dr H. Smith at the early stages of this work, and helpful discussions with Dr J. Collett at the later stages. We are grateful to Dr L. Hernquist for providing us with his galaxy generation code. We thank Drs S. Dutta, K. Holley-Bockelmann and Mr I. Berentzen for giving us companion galaxy generation programs, and acknowledge the referee, Dr J. Barnes, for comments that greatly improved the paper. We thank Drs S. Vogel, M. Regan, J. Kenney and J. Knapen for providing us with Hα data, and Drs M. Prieto, P. Martin and D. Friedli for giving us optical images of NGC 7479. We are grateful for a time allocation on the University of Kiel GRAPE (DFG Sp345/5). CH acknowledges support from DFG grant Fr 325/39-1-2.

REFERENCES

Abraham R. G., Tanvir N. R., Santiago B. X., Ellis R. S., Glazebrook K., van den Bergh S., 1996a, MNRAS, 279, L47
Abraham R. G., van den Bergh S., Glazebrook K., Ellis R. S., Santiago B. X., Surma P., Griffiths R. E., 1996b, ApJS, 107, 1
Ashman K. M., 1992, PASP, 104, 1109
Barnes J. E., Hernquist L., 1996, ApJ, 471, 115
Bekki K., 1998, A&A, 334, 814
Binney J., Tremaine S., 1987, Galactic Dynamics. Princeton Univ. Press, Princeton, NJ
Blackman C. P., 1983, MNRAS, 202, 379
Carlberg R. G., Freeman W. L., 1985, ApJ, 298, 486
de Vaucouleurs G., 1948, Ann. d'Astrophys, 11, 247
de Vaucouleurs G., de Vaucouleurs A., Corwin H. G. Jr., Buta R. J., Paturel G., Fouqué P., 1991, Third Reference Catalogue of Bright Galaxies. Springer, New York
Devereux N. A., 1989, ApJ, 346, 126
Earn D. J. D., 1993, PhD thesis, Univ. Cambridge
Friedli D., Benz W., 1993, A&A, 268, 65
Friedli D., Benz W., 1995, A&A, 301, 649
Hasan H., Norman C., 1990, ApJ, 361, 69
Heller C. H., 1991, PhD thesis, Yale University
Heller C. H., Shlosman I., 1994, ApJ, 424, 84
Hernquist L., 1990, ApJ, 356, 359
Hernquist L., 1993, ApJS, 86, 389
Hernquist L, Mihos J. C., 1995, ApJ, 448, 41 (HM95)
Howard S., Byrd G. G., 1990, AJ, 99, 1798
Howard S., Keel W. C., Byrd G. G., Jordan B., 1993, ApJ, 417, 502
Huchtmeier W. K., Richter O.-G., 1989, A General Catalog of H I Observations of Galaxies. Springer-Verlag, New York
Keel W. C., 1983, ApJS, 52, 229
King I. R., 1966, AJ, 71, 64
Kuzmin G., 1956, AZh, 33, 27
Laine S., 1996, PhD thesis, Univ. Florida
Laine S., Gottesman S. T., 1998, MNRAS, 297, 1041
Laine S., Shlosman I., Heller C. H., 1998, MNRAS, 297, 1052
Laine S., Kenney J. D. P., Yun M. S., Gottesman S. T., 1999, ApJ, 511, 709
Martin P., 1995, AJ, 109, 2428
Martin P., Friedli D., 1997, A&A, 326, 449
Martinet L., 1995, Fundam. Cosmic Phys., 15, 341
Mihos J. C., Bothun G. D., 1997, ApJ, 481, 741
Mihos J. C., Hernquist L., 1994, ApJ, 425, L13
Mihos J. C., Walker I. R., Hernquist L., Mendes de Oliveira C., Bolte M., 1995, ApJ, 447, L87
Monaghan J. J., 1992, ARA&A, 30, 543
Morgan I., Smith R. M., Phillipps S., 1998, MNRAS, 295, 99
Nilson P., 1973, Uppsala General Catalogue of Galaxies. Royal Soc. Sci., Uppsala, Sweden
Norman C. A., Sellwood J. A., Hasan H., 1996, ApJ, 462, 114
Odewahn S. C., 1994, AJ, 107, 1320
Odewahn S. C., 1996, in Buta R., Crocker D. A., Elmegreen B. G., eds, Proc. IAU Colloq. 157, ASP Conf. Ser. Vol. 91, Barred Galaxies. Astron. Soc. Pac., San Fransisco, p. 30
Ostriker J. P., Peebles P. J. E., 1973, ApJ, 186, 467
Phillips A. C., 1996, in Buta R., Crocker D. A., Elmegreen B. G., eds, Proc. IAU Colloq. 157, ASP Conf. Ser. Vol. 91, Barred Galaxies. Astron. Soc. Pac., San Fransisco, p. 44
Phookun B., 1993, PhD thesis, Univ. Maryland
Phookun B., Mundy L. G., 1995, ApJ, 453, 154
Phookun B., Mundy L. G., Teuben P. J., Wainscoat R. J., 1992, ApJ, 400, 516
Phookun B., Vogel S. N., Mundy L. G., 1993, ApJ, 418, 113
Quillen A., Frogel J. A., Kenney J. D. P., Pogge R. W., DePoy D. L., 1995, ApJ, 441, 549
Quinn P. J., Hernquist L., Fullagar D. P., 1993, ApJ, 403, 74

Salo H., Byrd G., 1994, in I. Shlosman, ed., Mass-Transfer Induced Activity in Galaxies. Cambridge Univ. Press, Cambridge, p. 412

Sandage A., Tammann G. A., 1987, A Revised Shapley–Ames Catalog of Bright Galaxies, 2nd edition, Carnegie Inst., Washington DC

Schechter P., 1976, ApJ, 203, 297

Sofue Y., 1994, ApJ, 423, 207

Steinmetz M., 1996, MNRAS, 278, 1005

Sugimoto D., Chikada Y., Makino J., Ito T., Ebisuzaki T., Umemura M., 1990, Nat, 345, 33

Thakar A. R., Ryden B. S., 1996, ApJ, 461, 55

Thakar A. R., Ryden B. S., 1998, ApJ, 506, 93

Theis C., 1998, Rev. Mod. Astron., 12

Toomre A., 1963, ApJ, 138, 385

Toomre A., 1981, in Fall S. M., Lynden-Bell D., eds, The Structure and Evolution of Normal Galaxies. Cambridge Univ. Press, Cambridge, p. 111

Tóth G., Ostriker J. P., 1992, ApJ, 389, 5

Tully R. B., 1988, Nearby Galaxies Catalog, Cambridge Univ. Press, Cambridge

van den Bergh S., Abraham R. G., Ellis R. S., Tanvir N. R., Santiago B. X., Glazebrook K. G., 1996, AJ, 112, 359

Walker I. R., Mihos J. C., Hernquist L., 1996, ApJ, 460, 121

Whitehurst R., 1988, MNRAS, 233, 529

Young J. S., Xie S., Kenney J. D. P., Rice W. L., 1989, ApJS, 70, 699

Zaritsky D., Rix H.-W., 1997, ApJ, 477, 118

Zaritsky D., Smith R., Frenk C., White S. D. M., 1993, ApJ, 405, 464

Zaritsky D., Smith R., Frenk C., White S. D. M., 1997, ApJ, 478, 39

This paper has been typeset from a TEX/LATEX file prepared by the author.